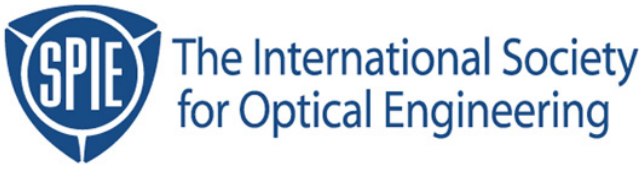

This paper was published in the proceedings of
Lithography for Semiconductor Manufacturing
SPIE Vol. 3741, pp. 148-160.

Effect of Developer Temperature and Normality on Conventional and Chemically Amplified Photoresist Dissolution

Chris A. Mack[1], Mark John Maslow[1], Jeffrey Byers[2]

[1]*FINLE Technologies Inc., P.O. Box 162712, Austin TX, 78716*
[2]*International SEMATECH, 2706 Montopolis Dr., Austin, TX 78741*
email: chris_mack@finle.com

ABSTRACT

The effects of developer temperature on several conventional resists and one chemically amplified resist, and the effects of developer normality on the dissolution behavior of a 248nm chemically amplified resist, are examined using development rate measurements. Using an RDA-790 development rate measurement tool, dissolution rates as a function of dose and depth into the resist were measured. Each data set was analyzed and the performance of rate versus dissolution inhibitor concentration was fit to appropriate models. The variation of these results with developer temperature has led to temperature-dependent characterization of the dissolution modeling parameters. The variation of dissolution rate with developer normality has led to an initial characterization of the normality-dependent dissolution modeling parameters.

Keywords: Photoresist Development, Developer Temperature, Developer Normality, Lithography Simulation, PROLITH

1. INTRODUCTION

It has been shown previously that there is significant impact of developer temperature on resist performance [1]. The previous work has produced a well-understood model for the behavior of the temperature dependence of conventional photoresist dissolution rates. As the industry continues to advance chemically amplified resist technology, the behavior of these new resists under varying developer temperatures and developer normalities is less understood.

This paper will analyze the effects of developer temperature and developer normality on the dissolution rate of several conventional and one chemically amplified resist. Using the RDA-790 development rate monitor [2,3], dissolution rate as a function of dose and depth into resist was measured. Each data set was analyzed and the basic performance of dissolution rate versus inhibitor concentration was fit to mathematical models. The variation of the dissolution rate with developer temperature and developer normality has lead to an initial temperature-dependent, normality-dependent characterization of dissolution modeling parameters for APEX-E chemically amplified resist, and temperature-dependent characterization of dissolution modeling parameters for several g-line and i-line resists.

Once models have been established for the temperature and normality dependence of the dissolution behavior, comprehensive simulated experiments, not practical in a laboratory setting, can be performed. The results will lead to improved models that allow the optimization of developer temperature and developer normality for advanced processes.

2. THEORY

The dissolution rate of a photoresist as a function of exposure dose is often characterized by fitting the response to a model. If the model adequately describes the shape of the actual data, the parameters of the model will provide a compact representation of the dissolution rate behavior. For example, the dissolution rate of a photoresist, *R*, as a function of the relative photoactive compound (PAC) concentration (the dissolution inhibitor), *m*, can often be fit well with the four-parameter Mack kinetic model [4]:

$$R(m) = R_{\max}\frac{(a+1)(1-m)^n}{a+(1-m)^n} + R_{\min} \qquad (1)$$

where R_{max} is the maximum (fully exposed) dissolution rate, R_{min} is the minimum (unexposed) dissolution rate, n is the dissolution selectivity (which corresponds to the surface reaction order), and a is a simplifying constant given by

$$a = \frac{(n+1)}{(n-1)}(1-m_{TH})^n$$

and where m_{TH} is the threshold PAC concentration, defined as the point of inflection of the *R(m)* curve. Here, unexposed resist dissolution (given by R_{min}) is assumed to occur by a separate mechanism from exposed dissolution. In some cases, m_{TH} takes on a large negative value and a becomes large. In this case, the dissolution model simplifies to

$$R = R_{\max}(1-m)^n + R_{\min} \qquad (2)$$

Other models are also possible, such as the enhanced kinetic model proposed by Mack [5] and the "notch" model of Mack and Arthur [6]. The notch model is especially effective in describing many of today's most advanced resists. This notch model begins with the simple version of the Mack model given in equation (2) and adds a notch function equivalent to the threshold behavior given by equation (1).

$$R = R_{\max}(1-m)^n\left[\frac{(a+1)(1-m)^{n\_notch}}{a+(1-m)^{n\_notch}}\right] + R_{\min} \qquad (3)$$

where

$$a = R_{\max}\frac{(n\_notch+1)}{(n\_notch-1)}(1-m_{TH\_notch})^{n\_notch}$$

The term in the brackets of equation (3) provides the notch-like behavior where m_{TH_notch} is the position of the notch along the PAC concentration axis and *n_notch* gives the strength of the notch. Note that the five parameter notch model of equation (3) reverts to the original Mack model of equation (1) when $n = 0$ and becomes equivalent to the simplified Mack model of equation (2) when *n_notch* = 1.

The effect of temperature on dissolution rate has been studied previously [1]. The results show a complicated behavior where changes in developer temperature produce changes in dissolution rate that are dose dependent. Thus, at one dose the effect of temperature on dissolution rate can be very different than at another dose. Use of a dissolution rate model can simplify the description of temperature and normality effects by showing just the change in the model parameters with developer temperature and normality.

3. EXPERIMENTAL

One *g*-line and seven *i*-line photoresists were studied in order to understand the impact of developer temperature on dissolution rate behavior. The *g*-line resist OFPR-800 is one of the oldest photoresists still in use in the semiconductor industry and is known as a low contrast resist. THMR-iP3650 by TOK, SPR505 by Shipley, SPR510L, a dyed version of 505, and Clariant's AZ7518 are mid-contrast *i*-line resists in common use. TOK's TDMR-AR80, Shipley's SPR955, and JSR's PFR-iX1040G are state-of-the-art high contrast *i*-line resists. Each resist was coated on bare silicon wafers to thicknesses of about 0.6 – 1.8 μm. The softbake and post-exposure bake (PEB) conditions for each resist, as well as the specific developer used, are given in Table I. All developers are TMAH-based. One chemically amplified resist, Shipley's APEX-E, was used. Application, exposure, and PEB of this resist was performed using SEMATECH's standard process flow for APEX-E with the wafers going through PEB immediately following exposure.

Dissolution rates were measured using an RDA-790 resist development analyzer manufactured by Litho Tech Japan. The system uses a measurement head with 18 channels to provide reflectance interferometry on 18 exposure sites on the wafer simultaneously. The resulting reflectance versus time signals are converted to resist thickness versus time and finally development rate versus thickness using the tool's built-in LEAPSET software. The RDA-790 is equipped with a NESLAB RTE-111 constant temperature bath that provides better than 0.02ºC control of the developer temperature for immersion-mode (agitated with a magnetic stirrer) dissolution rate measurements. Developer can be pumped directly into the immersion tank or can be hand-poured.

All resists were measured at developer temperatures from 14ºC to 30ºC in 2ºC increments, except SPR505, SPR955, AZ7518 and APEX-E which used an extended range of 5ºC to 45ºC in 5ºC increments. For the normality measurements with APEX-E, CD-26 was diluted to run at normalities from 0.13 to 0.26. The data was then analyzed in the ProDRM software package [7] to convert the rate versus incident dose and depth in the resist, $R(E,z)$, into rate versus PAC concentration (or *t*-BOC concentration in the case of APEX-E), $R(m)$, and then fit to a development model. The original Mack model of equation (1) was found to give good fits to all data sets, with the exception of the notch behavior exhibited by the three high contrast i-line resists as described below.

Table I. Processing conditions for each resist.

Resist	Softbake Temp. (ºC)	Softbake Time (sec)	PEB Temp. (ºC)	PEB Time (sec)	Developer
OFPR-800	90	60	none	none	NMD-W
THMR-iP3650	90	90	110	90	NMD-W
SPR505	95	60	115	60	MIF702
SPR510L	95	60	115	60	MIF702
AZ7518	95	60	115	60	NMD-W
SPR955	95	60	115	60	NMD-W
TDMR-AR80	90	90	110	90	NMD-W
PFR-iX1040G	90	120	110	90	NMD-W
APEX-E	90	60	90	60	CD-26

4. RESULTS

4.1 Developer Temperature Effects – Conventional Resists

The variation of the dissolution rate behavior with developer temperature was similar for all resists but of greater or lesser degree depending on the resist. Typical dissolution measurements are illustrated in Figure 1. At a given depth into the resist (in this case, the middle 20% of the resist was used), the development rate as a function of incident dose can be plotted in a characteristic Hurter-Driffield like curve, as shown in Figure 2a. In general, one usually expects simple kinetic rate limited reactions to proceed faster at higher temperatures (indicating a positive activation energy for the reaction). The behavior shown in Figure 2a is obviously more complicated than that. At high doses, increasing developer temperature does increase the development rate. But at low doses the opposite is true. Thus, developer temperature has a significant impact on the shape of the dissolution rate curve, that is, on the resist contrast.

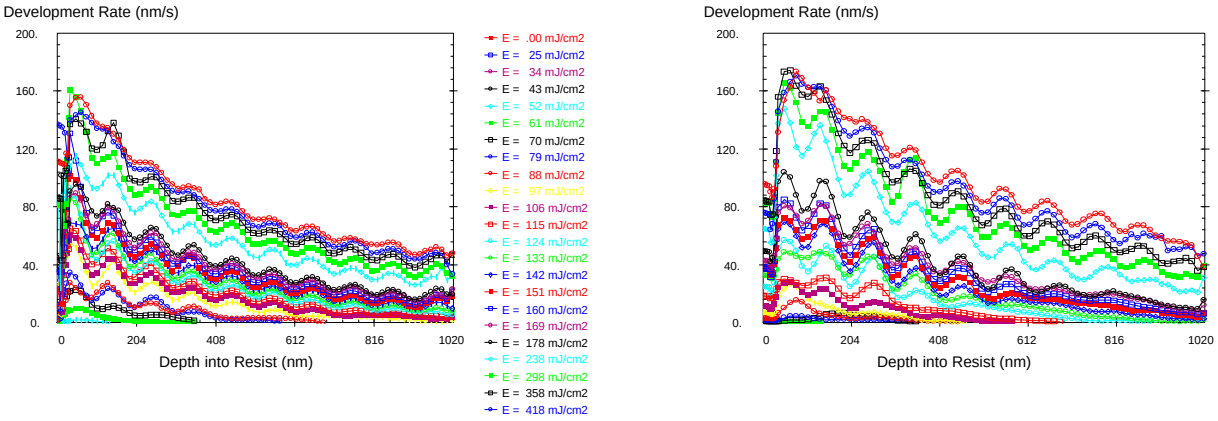

(a) (b)

Figure 1. Dissolution rate data from the RDA-790 for THMR-iP3650 at developer temperatures of (a) 14°C and (b) 30°C.

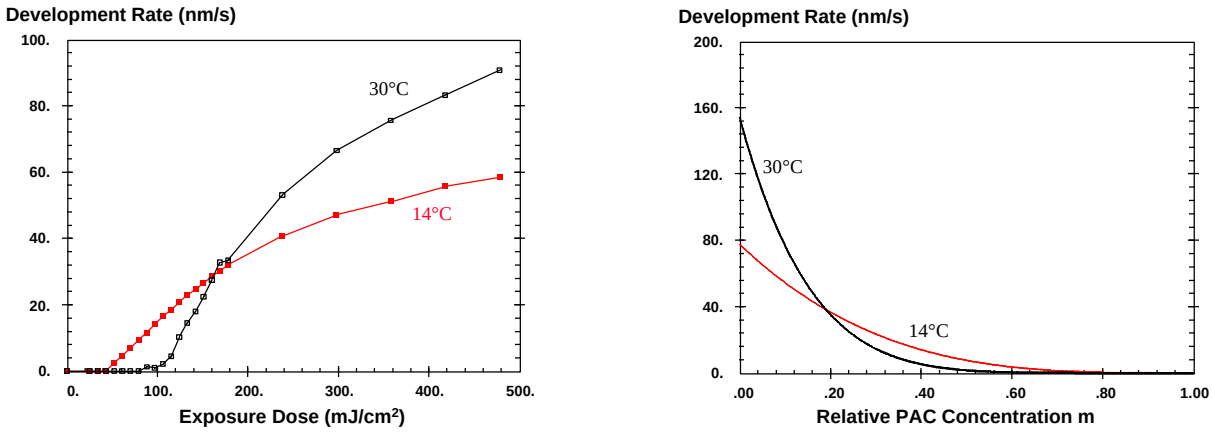

(a) (b)

Figure 2. Development rate of THMR-iP3650 (a) as a function of exposure dose, and (b) as a function of PAC concentration for different developer temperatures, showing a change in the shape of the development response to exposure.

By fitting the dissolution rate behavior to a development model, the variation of the *R(m)* curve with temperature can be shown, as in Figure 2b. For this fitting, the top portion of the resist was excluded in order to eliminate surface inhibition effects and analyze only the bulk development behavior. Again, the results show that at high doses (corresponding to low concentrations of photoactive compound remaining) higher developer temperature increases the development rate. But at low doses (high concentrations of photoactive compound remaining), the opposite is true. Using the terminology of the Mack development model, increasing the developer temperature caused an increase in the maximum development rate R_{max} and an increase in the dissolution selectivity parameter *n*. The threshold PAC concentration m_{TH} was found to be negative for most of the conventional resists studied (and in the 0.0 – 0.15 range for a few) and did not vary significantly with temperature. Measurement of R_{min} exclusive of the surface inhibition effect requires special care and was not attempted in this study. The data showed that R_{min} was quite small for all resists (except OFPR-800) over the full temperature range.

Figure 3 shows the final results of the analysis for one resist. The two parameters R_{max} and *n* are plotted versus developer temperature for each resist in an Arrhenius plot. Several resists exhibited significant standing waves for the conditions used and as a result showed somewhat noisier data than others. The activation energies and Arrhenius coefficients resulting from the fits of this data are given in Table II for R_{max} and Table III for the dissolution selectivity parameter *n*.

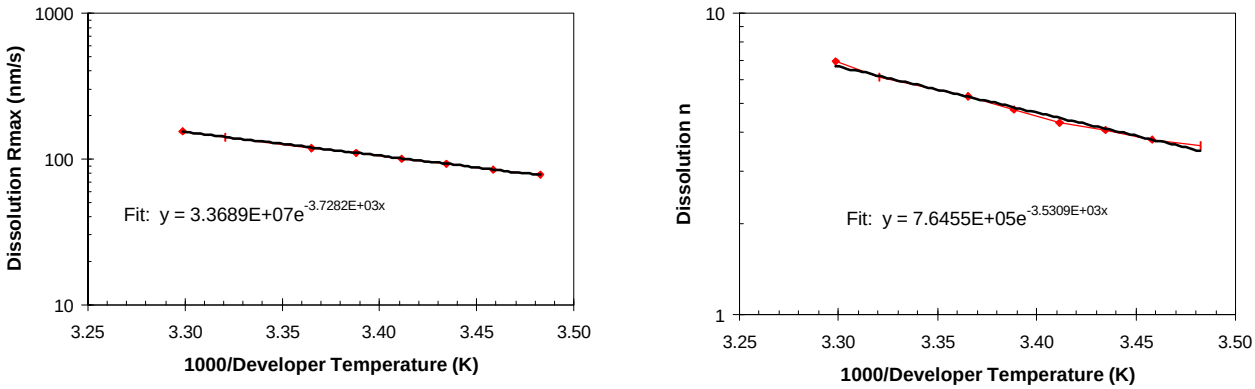

(a) (b)

Figure 3. Arrhenius plots of (a) the maximum dissolution rate R_{max} and (b) the dissolution selectivity parameter *n* for THMR-iP3650. Best fits to the Arrhenius equation are also shown.

The three high contrast resists, SPR955, TDMR-AR80, and PFR-iX1040G, each exhibited a dissolution notch over part or all of the temperature range studied. It appeared as if the strength of the notch varied with temperature. However, accurate characterization of the notch, which requires dissolution rate measurements concentrated at doses near the notch position, was not carried out.

Examination of the data in Tables II and III shows that different resist have very different sensitivities to developer temperature. All of the resists showed basic Arrhenius behavior over the temperatures ranges studied except SPR505, which seemed to saturate at temperatures above 30ºC. The activation energies for R_{max} for all resists were in the range of 5.1 – 8.8 Kcal/mole (an activation energy of E_a = 8 Kcal/mole means that R_{max} will approximately double over the temperature range of 15 – 30ºC; an activation energy of 5 Kcal/mole will increase R_{max} by about 50% over the same range). The impact of developer temperature on the dissolution selectivity

parameter *n* was much more varied. AZ7518 showed virtually no temperature dependence with respect to *n* (E_a = 0.767 Kcal/mole) while PFR-iX1040G showed a tripling of the value of *n* as the temperature varied from 15 to 30ºC (E_a = 12.65 Kcal/mole).

Table II. Results of the fit of R_{max} to an Arrhenius relationship.

Resist	Activation Energy (Kcal/mol)	Arrhenius Coefficient (nm/s)	ln(Ar)
OFPR-800	5.32	7.084×10^{5}	13.47
THMR-iP3650	7.41	3.368×10^{7}	17.33
SPR510L	5.12	2.895×10^{5}	12.58
SPR505	2.33 (5.16)[a]	2.084×10^{3} (5.40×10^{4})[a]	7.64 (10.90[a])
AZ7518	6.14	5.198×10^{6}	15.46
SPR955	5.14	7.986×10^{5}	13.59
TDMR-AR80	8.75	3.384×10^{8}	19.64
PFR-iX1040G	8.43	1.796×10^{8}	19.01

Notes: a) results of Arrhenius fit if only the 10 – 30ºC temperature range is used.

Table III. Results of the fit of *n* to an Arrhenius relationship.

Resist	Activation Energy (Kcal/mol)	Arrhenius Coefficient (nm/s)	ln(Ar)
OFPR-800	2.26	5.998×10^{1}	4.09
THMR-iP3650	7.02	7.65×10^{5}	13.55
SPR510L	4.57	6.092×10^{3}	8.71
SPR505	5.19	5.398×10^{4}	10.90
AZ7518	0.767	1.132×10^{1}	2.42
SPR955	3.57	1.304×10^{3}	7.17
TDMR-AR80	10.31	2.824×10^{8}	19.46
PFR-iX1040G	12.65	1.627×10^{10}	23.51

4.2 Developer Temperature Effects – APEX-E

All data collected for the developer temperature study for APEX-E used Shipley CD-26 developer at 0.26N. The variation of the dissolution behavior with developer temperature was similar to previously shown i-line resists. These previously studied resists showed a negative m_{TH} value allowing use of the simplified model in

equation (2). APEX-E exhibited a positive m_{TH} value, shown to have a small dependence on the developer temperature.

This analysis of the bulk development behavior shows that as temperature increases, the maximum development rate (R_{max}) increases. At lower doses (higher concentrations of PAC) a shift in the threshold PAC concentration m_{TH} and an increase in the dissolution parameter n result in more complicated dissolution rate behavior. Measuring R_{min} without including surface effects requires considerable care and was not attempted in this work. Simple R_{min} calculations were performed on unexposed sites by measuring resist thickness before and after development.

Figure 4 shows the final results of the analysis. All four parameters of the original Mack model of dissolution are plotted versus developer temperature in an Arrhenius plot. Dissolution parameters R_{min} and n go through behavior that cannot be accurately explained with Arrhenius plots at high developer temperature. Dissolution parameter R_{max} is described using two different Arrhenius fits. The break point occurs between developer temperatures of 30º and 35ºC. Table IV shows the activation energies and Arrhenius coefficients resulting from the fit of this data and Table V shows the development rate parameters at each temperature.

Table IV. Results of the fit of all dissolution parameters to an Arrhenius Relationship.

Develop Parameter	Activation Energy (Kcal/mol)	Arrhenius Coefficient	ln(Ar)
R_{max} [a]	8.2 / 0.9324	1.49×10^{8} / 903.22	18.42 / 6.81
R_{min} [b]	2.1779	61.257	4.12
m_{TH} [b]	0.0467	0.5673	-0.57
n [b]	3.2174	1262.5	7.14

Notes: a) R_{max} values for the two fits of the separate regions. Region 1: 5ºC - 30ºC Region 2: 35ºC - 45ºC
b) Results of fit using a temperature range of 5ºC - 30ºC

Table V. Developer Temperature Dependent Modeling Parameters of APEX-E (0.26N developer)

Developer Temperature	R_{max} (nm/s)	R_{min} (nm/s)	m_{TH}	n
5° C	53.14 ± 8.96	1.176	0.571 ± 0.036	3.931 ± 0.556
10° C	67.97 ± 10.87	1.2833	0.578 ± 0.031	4.169 ± 0.519
15° C	91.93 ± 13.81	1.349	0.586 ± 0.028	4.250 ± 0.485
20° C	115.66 ± 14.1	1.482	0.682 ± 0.016	4.786 ± 0.488
25° C	146.05 ± 15.21	1.554	0.637 ± 0.015	5.562 ± 0.544
30° C	177.83 ± 15.99	1.621	0.646 ± 0.012	6.355 ± 0.554
35° C	199.65 ± 14.56	2.562	0.693 ± 0.008	15.578 ± 2.171
40° C	196.17 ± 13.14	2.135	0.694 ± 0.008	11.247 ± 1.321
45° C	209.54 ± 22.52	1.834	0.665 ± 0.014	6.642 ± 0.736

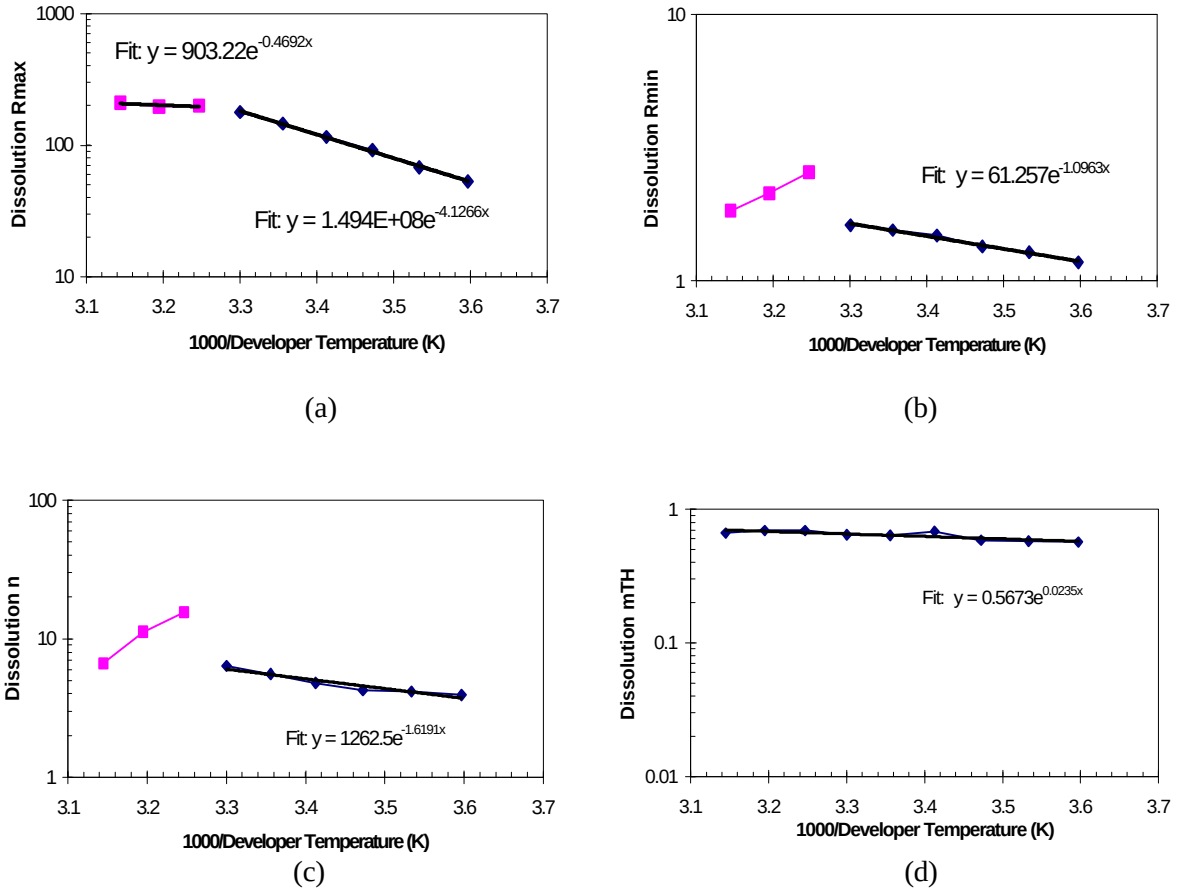

Figure 4. Arrhenius plots of (a) the maximum dissolution rate R_{max}, (b) the minimum dissolution rate R_{min}, (c) the dissolution selectivity parameter n, and (d) the threshold PAC concentration m_{TH}. Best fits to the Arrhenius equation are also shown.

4.3 Developer Normality Effects – APEX-E

The data for the study of the effect of developer normality was collected using Shipley CD-26 developer, diluted to 0.13, 0.195, 0.24425 and full strength (0.26) normalities at 20ºC, 35ºC, and 40ºC developer temperatures. The variation of the dissolution rate behavior with developer normality was similar to the variation with developer temperature. In general, one expects kinetic rate limited reactions to proceed slower at lower normalities. As can be seen in Figure 5, at a given depth into the resist (again, the middle 20% of the resist was used) the development rate is slowed for all exposure energies as the normality is decreased. Data collected at 0.13 N did not see sufficient dissolution to be included in the full analysis.

The analysis of the bulk development behavior shows that as normality decreases, the maximum development rate (R_{max}) decreases. At lower doses (higher concentrations of PAC) a shift in the threshold PAC concentration m_{TH}, and a decrease in the dissolution parameter n result in more complicated dissolution rate behavior. Measuring R_{min} without including surface effects requires considerable care and was not attempted. Simple R_{min} calculations were performed on unexposed sites measured before and after development.

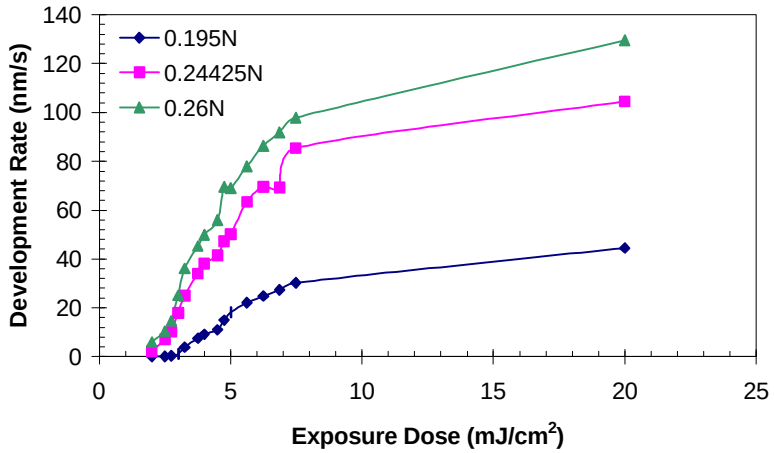

Figure 5. Development rate of APEX-E (averaged through the middle 20% of the resist thickness) as a function of exposure dose for different developer normalities at a developer temperature of 20ºC. At all doses, lower developer normality decreases the dissolution rate, with higher doses receiving the greatest decrease. Lower developer normality also decreases the dissolution selectivity parameter *n*.

Figure 6 shows the final results of the analysis. The original Mack model parameters R_{max} and the dissolution selectivity parameter *n* are shown to vary with developer normality. As the developer temperature increases, the impact of different developer normalities on R_{max} is lessened. The impact of normality on the dissolution selectivity *n* is quite complicated. Development modeling parameters for each normality are given in Table VI.

Table VI. Developer Normality Dependent Modeling Parameters for APEX-E

Developer Temperature	Developer Normality	R_{max} (nm/s)	R_{min} (nm/s)	m_{TH}	*n*
20°C	0.195	45.88 ± 7.93	0.272	0.527 ± 0.03	5.263 ± 1.002
20°C	0.24425	90.93 ± 11.27	0.9121	0.607 ± 0.018	5.408 ± 0.607
20°C	0.26	115.66 ± 14.1	1.482	0.682 ± 0.016	4.786 ± 0.488
35°C	0.195	78.08 ± 12.91	0.3953	0.533 ± 0.01	17.329 ± 2.176
35°C	0.24425	151.33 ± 13.07	1.191	0.667 ± 0.008	11.091 ± 1.14
35°C	0.26	199.65 ± 14.56	2.562	0.693 ± 0.008	15.578 ± 2.171
40°C	0.195	118.49 ± 94.6	0.3953	0.511 ± 0.074	8.715 ± 1.925
40°C	0.24425	182.86 ± 12.36	1.473	0.675 ± 0.005	16.441 ± 1.617
40°C	0.26	196.17 ± 13.14	2.135	0.694 ± 0.008	11.247 ± 1.321

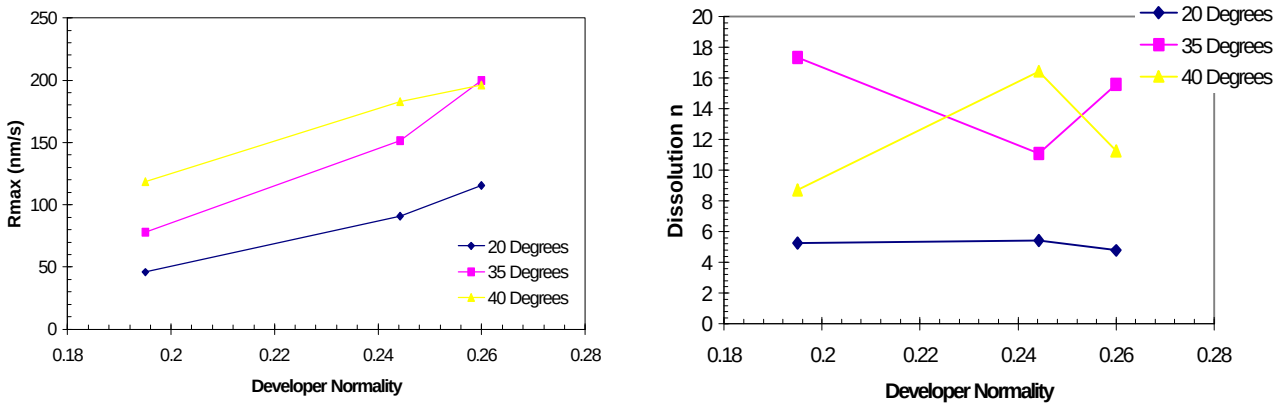

(a) (b)

Figure 6: Plots of (a) the maximum dissolution rate R_{max}, and (b) the dissolution selectivity parameter n versus developer normality for different developer temperatures.

5. SIMULATION RESULTS

What is the lithographic impact of these changes in dissolution rate behavior? An advantage of describing the effects of developer temperature and normality as a variation in modeling parameters is the ease with which simulation can be employed to explore their impact. For example, does a resist get "faster" or "slower" as developer temperature is increased? If the "speed" of a photoresist is judged by its dose-to-clear (E_o) or its dose-to-size (E_S), it is not clear at first glance how the changes in development rate response shown above will affect resist speed. Using the lithography simulator PROLITH/2 [8], dose-to-clear and dose-to-size were simulated for THMR-iP3650 as a function of developer temperature. Figure 7 confirms the well-known result that colder developer results in a faster resist. This seemingly counter-intuitive result is explained by the increasing value of the dissolution selectivity parameter n with developer temperature.

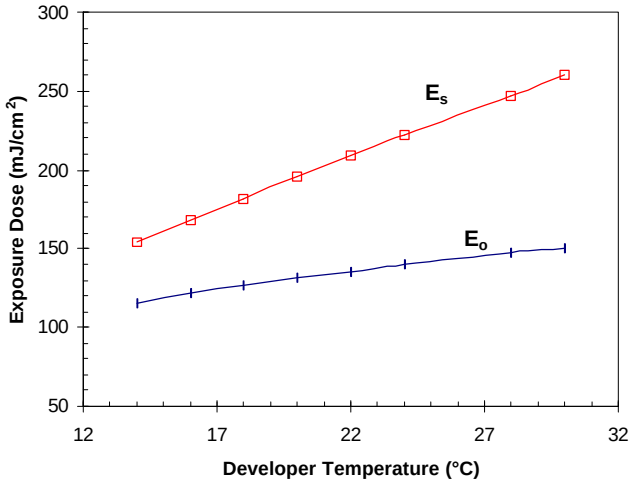

Figure 7. Simulated results of dose-to-clear (E_o) and dose-to-size (E_s) as a function of developer temperature for THMR-iP3650.

Another valuable use of modeling is investigating the sensitivity of these resists to developer temperature variations. Figure 8 shows how two different resists will behave in the presence of temperature errors by plotting the resulting change in resist linewidth.

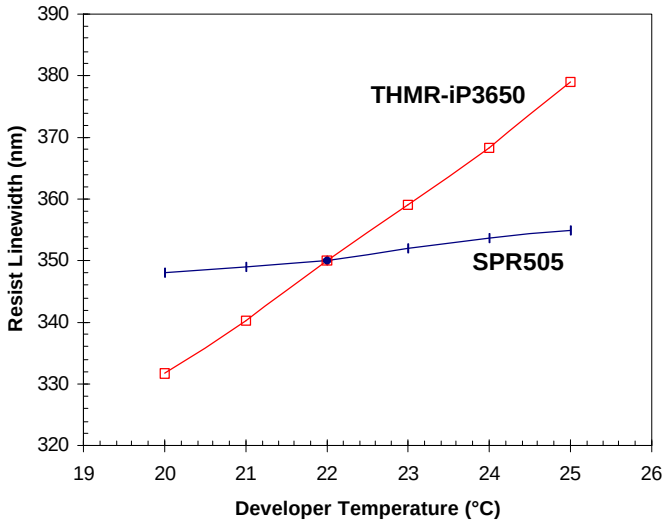

Figure 8. Simulated results of resist linewidth as a function of developer temperature for two resists.

The standard process flow for APEX-E at SEMATECH calls for Shipley MF-702 (0.21N) developer at room temperature (22°C) for 84 seconds. The modeling parameters measured for MF-702 at 20°C were measured and are shown in Table VII. Simulations of a binary 200nm line/space pattern were performed using PROLITH/2. At best focus, the standard process resist profile is shown in Figure 9. In comparison, the resist profile at best focus using the modeling parameters for a 35°C, 0.195N develop process is shown in Figure 10. The only changes made were to the dose to size and the parameters of the develop model.

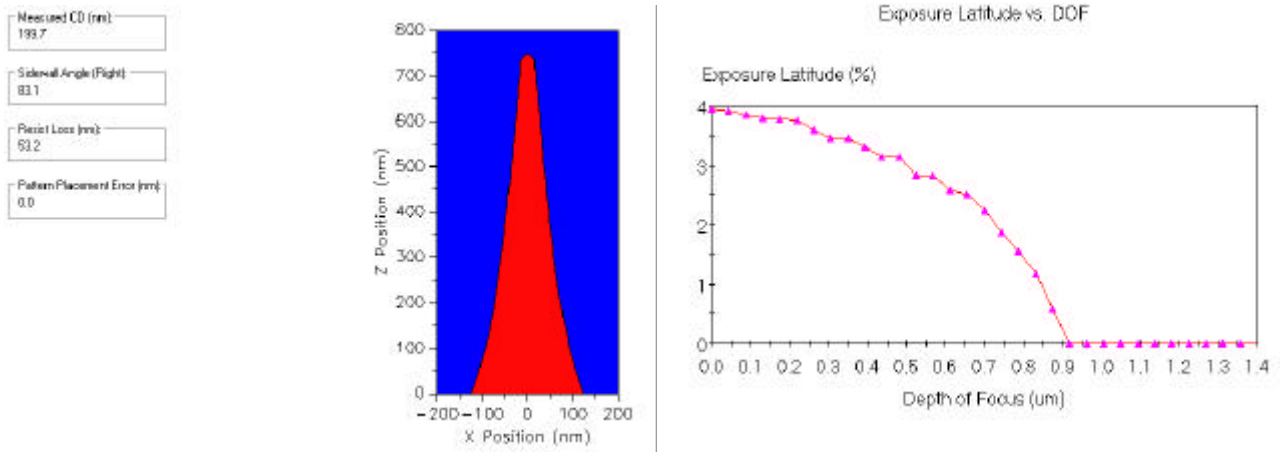

(a) (b)

Figure 9. PROLITH simulated (a) resist profile for a binary 200nm line/space feature using MF-702 Developer at 20°C, and (b) Exposure Latitude vs. DOF analysis of a Focus-Exposure Matrix.

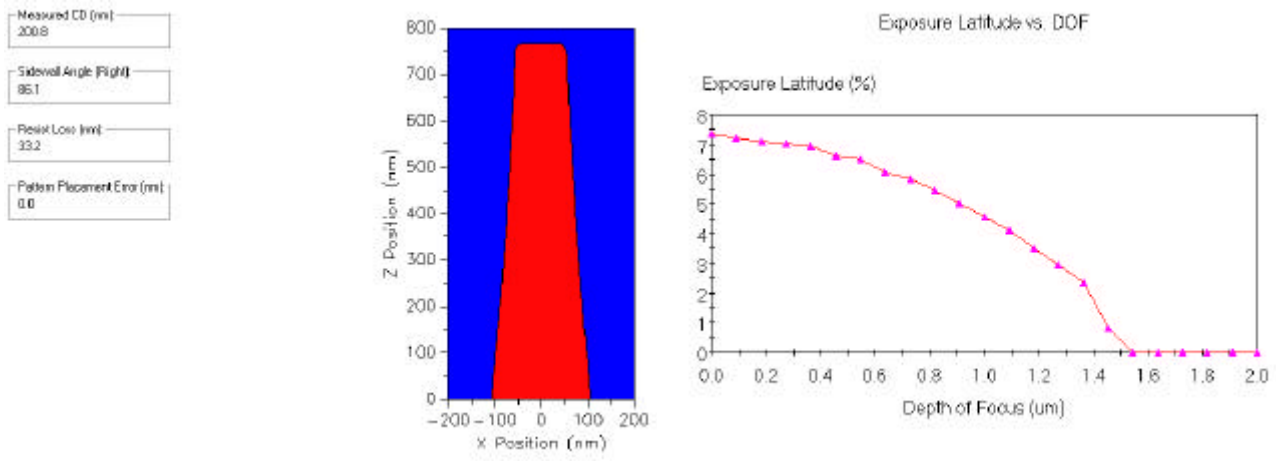

(a) (b)

Figure 10. PROLITH simulated (a) resist profile for a binary 200nm line/space feature using CD-26 developer (diluted to 0.195N) at 35°C, and (b) Exposure Latitiude vs. DOF analysis of a Focus-Exposure Matrix.

Table VII. MF-702 (20°C) Developer Modeling Parameters for APEX-E

R_{max} (nm/s)	64.54 ± 9.48
R_{min} (nm/s)	0.397
m_{TH}	0.577 ± 0.022
n	5.293 ± 0.842

6. CONCLUSIONS

By parameterizing the effects of developer temperature and developer normality with the coefficients to a development model, one is able to characterize a complicated reaction in a relatively simple, straightforward manner. For the results studied here the Mack development model provided good fits to the experimental data over the full range of developer temperatures and normalities except for the highest contrast i-line resist, which required the notch model. All of the model parameters showed Arrhenius behavior with developer temperature to different degrees. For some resists, R_{max} had two distinct Arrhenius regions. For APEX-E, the non-Arrhenius behavior of R_{min} and n above 30ºC and the change in activation energy of R_{max} indicate a change in the reaction mechanism in this temperature range. The normality study showed similar results where stronger normal developers had the higher R_{max} values. The simulation results for high-temperature low-normality APEX-E development show that process improvements can be made with modifications to the developer temperature and normality conditions.

7. REFERENCES

1. C. A. Mack, M. J. Maslow, A. Sekiguchi, R. Carpio, "New Model for the Effect of Developer Temperature on Photoresist Dissolution," *Advances in Resist Technology and Processing XV, Proc.*, SPIE Vol. 3333 (1998) pp. 169-142.
2. Litho Tech Japan Corporation, 2-6-6-201, Namiki, Kawaguchi, Saitama 332, Japan.
3. A. Sekiguchi, C. A. Mack, Y. Minami, T. Matsuzawa, “Resist Metrology for Lithography Simulation, Part 2: Development Parameter Measurements,” *Metrology, Inspection, and Process Control for Microlithography X, Proc.*, SPIE Vol. 2725 (1996) pp. 49-63.
4. C. A. Mack, "Development of Positive Photoresist," *J. Electrochemical Society,* Vol. 134, No. 1 (Jan. 1987) pp. 148-152.
5. C. A. Mack, "New Kinetic Model for Resist Dissolution," *J. Electrochemical Society,* Vol. 139, No. 4 (Apr. 1992) pp. L35-L37.
6. C. A. Mack and G. Arthur, “Notch Model for Photoresist Dissolution,” *Electrochemcial and Solid State Letters*, Vol. 1, No. 2, (August, 1998) pp. 86-87.
7. FINLE Technologies, Inc., P.O. Box 162712 Austin, TX 78716.
8. C. A. Mack, Inside PROLITH: A Comprehensive Guide to Optical Lithography Simulation, FINLE Technologies (Austin, TX: 1997).